Surprising formation of quasi-stable Tc(VI) in high ionic strength alkaline media

Journal:	*Inorganic Chemistry Frontiers*
Manuscript ID	QI-RES-03-2018-000219.R1
Article Type:	Research Article
Date Submitted by the Author:	30-Apr-2018
Complete List of Authors:	Chatterjee, Sayandev; Pacific Northwest National Laboratory, Energy and Environment Directorate Hall, Gabriel; Pacific Northwest National Laboratory, Nuclear Chemistry and Engineering Group Johnson, Isaac; Pacific Northwest National Laboratory, Du, Yingge; Pacific Northwest National Laboratory, Environmental Molecular Sciences Laboratory Walter, Eric; Pacific Northwest National Laboratory, Environmental Molecular Sciences Laboratory Washton, Nancy; Pacific Northwest National Laboratory, Environmental Molecular Science laboratory Levitskaia, Tatiana; Pacific Northwest National Laboratory, Radiochemical Science and Engineering

Journal Name

ARTICLE

Surprising formation of quasi-stable Tc(VI) in high ionic strength alkaline media

Sayandev Chatterjee,*†[a] Gabriel B. Hall,†[a] Isaac E. Johnson,[a] Yingge Du,[c] Eric D. Walter,[b] Nancy M. Washton,[b] Tatiana G. Levitskaia*[a]

Despite decades of research, the reduction behavior of pertechnetate, TcO_4^-, is not well understood and represents one of the largest knowledge gaps in the transition metal series. Conventional wisdom presumes the reduction of TcO_4^- in aqueous systems to predominantly follow either a rapid two electron, or three electron process to form either a Tc^V or Tc^{IV} species. This study for the first time demonstrates the importance of the Tc^{VI} species through systematic charactization by multiple spectroscopic techniques. The reduction of TcO_4^- was examined in a matrix of 5 M $NaNO_3$ at 0 − 2 M NaOH. Results of the cyclic voltammetric evaluation of reduction to Tc^{VI}, Nernstian analysis of the visible spectroelectrochemical signal, and structural spectroscopic EPR and XPS analysis of the reduction product generated by bulk electrolysis consistently support an electron transfer stoichiometry corresponding to a 1 e- reduction. This Tc^{VI} species is markedly more stable than had been previously considered, with decomposition kinetics that correspond to a half-life of 1.91 ± 0.07 days, fully 6 orders of magnitude longer than previously reported for an aqueous solution. These results reveal the importance of a Tc^{VI} intermediate species in high ionic strength alkaline solutions and significantly contribute to the understanding of the mechanism of TcO_4^- reduction and formation of low-valent Tc species.

Introduction

The redox behavior of technetium is of interest to a broad scientific community in fields ranging from diagnostic imaging and radiopharmaceuticals,[1-7] biogeochemistry,[8-11] nuclear fuel reprocessing,[12,13] to environmental chemistry.[14-19] Advancement of the fundamental knowledge of technetium (Tc) is vital to address challenges in each of these fields. Thus better understanding technetium chemistry impacts the fundamental knowledge of chemistry and biology, protects human health and the environment, and will streamline remediation of legacy nuclear waste and strategies for processing and final disposition of used nuclear fuel. Despite the wide reach, Tc redox behavior is among the least studied of the transition metals; primarily due to the difficulty in studying an element with no stable isotopes.

The large range of oxidation states observed for the elements in the manganese triad, and the difference in redox behavior exhibited by Mn and Re make inference of Tc behavior from the other members of its triad unreliable, and distinctions of behavior in the sequence Mn-Tc-Re are of great fundamental interest.[2,20] Important fundamental questions remain about how electrochemical properties, solution structure and reactivity of Tc compare with the other two elements in the manganese triad. While all three elements in the triad exhibit a propensity to exist in dynamic equilibrium between multiple oxidation states ranging from +7 to 0 in aqueous matrices (+7 to -1 for Re and Tc in acidic media),[21-23] significant differences are observed in their redox behavior as demonstrated by representative Latimer diagrams (Figure 1).[24] Examination of the Latimer diagrams in acidic solutions shows dissimilar susceptibility of the Mn triad metals to hydrolysis and stability of various oxidation states. For example, Mn^{VI} and Tc^{VI} are both suggested to proceed through the form of HMO_4^-, while Re exists as the trioxide. However, at low oxidation states Tc and Re behave more similarly, bypassing the oxidation states of +II and +III and proceeding directly to the metal while Mn exhibits relative stability as Mn^{II}. This in turn impacts redox mobility and further contributes to the observed differences in the redox stability of the triad.

[a.] Energy and Environment Directorate, Pacific Northwest National Laboratory, Richland, Washington 99354, United States; email: Sayandev.Chatterjee@pnnl.gov, Tatiana.Levitskaia@pnnl.gov
[b.] Environmental Molecular Sciences Laboratory, Pacific Northwest National Laboratory, Richland, Washington 99354, United States
[c.] Physical and Computational Sciences Directorate, Pacific Northwest National Laboratory, Richland, Washington 99354
† Authors contributed equally to the work

Acidic (red, top):

$Mn^{VII}O_4^- \xrightarrow{0.90} HMn^{VI}O_4^- \xrightarrow{1.28} H_3Mn^VO_4^- \xrightarrow{2.90} Mn^{IV}O_2 \xrightarrow{0.95} Mn^{III} \xrightarrow{1.50} Mn^{II} \xrightarrow{-1.18} Mn^0$

Spanning: 1.51, 2.09, 1.23, 1.70

$Tc^{VII}O_4^- \xrightarrow{-0.57} Tc^{VI}O_4^{2-} \xrightarrow{1.39} Tc^{IV}O_2 \xrightarrow{0.27} Tc^0$; $Tc^{VII}O_4^- \xrightarrow{0.70} Tc^{VI}O_3 \xrightarrow{0.83} Tc^{IV}O_2$

$Re^{VII}O_4^- \xrightarrow{0.77} Re^{VI}O_3 \xrightarrow{0.40} Re^{IV}O_2 \xrightarrow{0.28} Re^0$; $Re^{VII}O_4^- \xrightarrow{0.51} Re^{IV}O_2$

Basic (blue, bottom):

$Mn^{VII}O_4^- \xrightarrow{0.56} Mn^{VI}O_4^{2-} \xrightarrow{0.27} Mn^VO_4^{3-} \xrightarrow{0.96} Mn^{IV}O_2 \xrightarrow{0.15} Mn^{III}_2O_3 \xrightarrow{-0.25} Mn^{II}(OH)_2 \xrightarrow{-1.56} Mn^0$

Spanning: 0.34, 0.62, -0.05, 0.60

$Re^{VII}O_4^- \xrightarrow{0.77} Re^{VI}O_3 \xrightarrow{0.40} Re^{IV}O_2 \xrightarrow{-1.25} Re^{III}_2O_3 \xrightarrow{-0.33} Re^0$
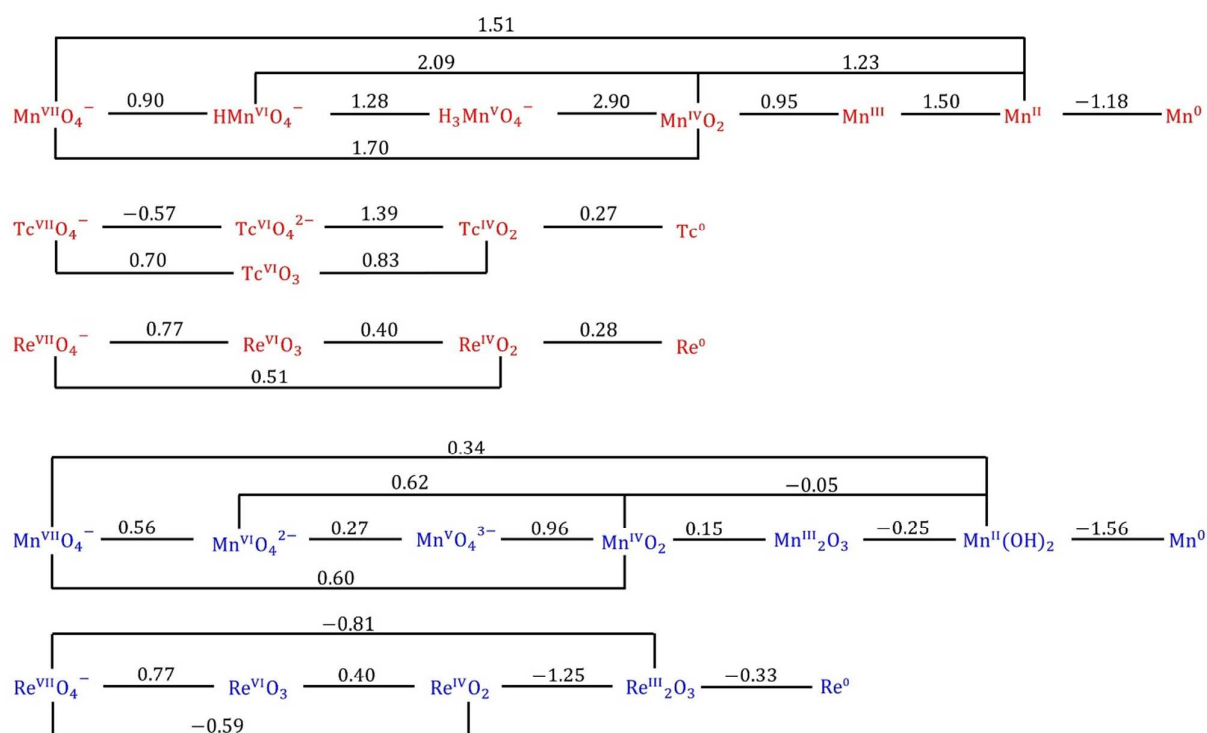
Spanning: -0.81, -0.59

Figure 1. Latimer diagram of the manganese triad for acidic (red, top), and basic (blue, bottom) conditions vs SHE.[24]

Particularly noteworthy is the dearth of thermodynamic data on Tc. In spite of observation of all the known Tc oxidation states in acidic media, only four make an appearance in the corresponding Latimer diagram in acidic solutions. This is a consequence of Tc redox being mostly irreversible and therefore not adequate for calculating thermodynamic data.[23,25,26] The scarcity is even more obvious for alkaline solutions where conflicting reports have prevented construction of a representative Latimer diagram. One key trend that is obvious from the Latimer diagrams of the triad is the general instability of the M(VI) species in aqueous solutions and their tendency to disproportionate therein. This in unison with the prevalent knowledge in Tc redox chemistry, which is based on studies performed in low to moderate ionic-strength solutions of neutral or alkaline pH, presumes reduction of TcO_4^- to follow rapid two or three electron pathways to form Tc(V) or Tc(IV); where Tc(VI) is formed only as an extremely short lived transient species or bypassed altogether. This paints an incomplete picture of Tc redox behavior that assumes aqueous Tc chemistry to be dominated primarily by Tc(VII) and Tc(IV) species irrespective of the electrolyte and solvent conditions, and the Tc(VI) and Tc(V) intermediates to have minimal impact in Tc redox and speciation. While the observation of Tc(VI) has been reported in aqueous solutions in several instances through electrochemical measurements, these species have at large shown instability and high propensity towards disproportionation. However, the present study will present evidence that in high ionic strength alkaline solutions, Tc(VI) is persistent at much longer time scales than previously thought.
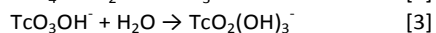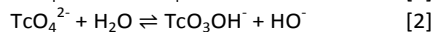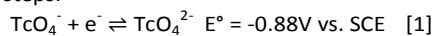
Expanding the literature search for Tc(VI) species to non-aqueous media does significantly improve the understanding of the stabilities and diversity of Tc(VI) species. Particularly in the presence of organic chelators, or in presence of π-donating ligands which stabilize the Tc(VI) oxidation state. The electrochemical reduction of TcO_4^- in organic media has shown stabilization of the Tc(VI) intermediate for long enough to allow for its first spectroscopic characterization.[27,28] It was also possible to isolate solid forms of the Tc(VI) species in an inert atmosphere, allowing for the confirmation of its molecular structure by X-ray powder diffraction and spectroscopic methods,[29] suggesting Tc(VI) as a relevant intermediate in TcO_4^- reduction. Tc(VI) halides of the form $TcCl_6$ and TcF_6 have been reported in the presence of a concentrated stream of X_2 gas,[30–33] while a nitrosylated version of the fluoride compound, $[(NO)_2TcF_8]$,[34] has also been reported. Colton and Tomkins[35] reacted thionyl chloride (an extremely strong Lewis acid) with NH_4TcO_4 to prepare the thionyl chloride adduct $(NH_4)_2[TcO_2Cl_4]SO_2Cl_2$. However, these compounds have shown a general tendency of limited stability and rapid disproportionation in aqueous media or even in the presence of moisture containing oxic environments. Tc (VI) oxo and nitrido halides are generally well represented in the literature,[22,35–45] but require the use of strong acids to be synthesized and stabilized in an aqueous environment. Chelating ligands have been shown to stabilize the Tc(VI) oxidation state with tris-bidentate alkoxo and thio compounds existing, in organic media.[46–49] The most persistent Tc(VI) complexes under mild conditions in the presence of water appear to be the dimeric μ-oxo aquanitrido complexes[50] and

nitrido amino carboxylate complexes,[51,52] the latter of which are stable at neutral pH.

While the general instability of Tc(VI) in aqueous media results in disproportionation a careful examination points to solvation water being a key offender in the disproportionation process. This is supported by (a) the Latimer diagram in acidic media showing formation of the hydrated Tc(VI) product, $Tc^{VI}O_4{}^{2-}$ being far less thermodynamically favorable compared to the anhydrous analog $Tc^{VI}O_3$; and (b)the observations of Tc (VI) oxo and nitrido halides requiring strong acids for their stabilization in aqueous environments.[22,35–45] Other observations of Tc(VI) species generated in literature also corroborates the adverse effect of solvation water on Tc(VI) disproportionation: while electrochemical reduction of TcO_4^- in aqueous chloride[53,54] or alkaline sulfate[55] matrices at low to moderate ionic strengths were observed to have a tendency to bypass the Tc(VI) oxidation state, voltammetric studies in strongly acidic (1-3 M H_2SO_4, 1 M $HClO_4$, 1 M HCl) or strongly alkaline (1 M NaOH) media, with much lower availability of solvation/hydration water, suggested the reduction proceeding through a Tc(VI) intermediate.[56] An additional contributing factor in the stabilization of the intermediate Tc(VI) species with increasing ionic strength may also be reduced O_2 solubility from air which can further resist its oxidation to Tc(VII). A notable observation comes in the form of coulometric generation of quasi-stable Tc(VI) species in the presence of gelatin.[57,58] The reason for the stabilization by gelatin is not entirely clear, but stabilization of the Tc(VI) state by coordination with peptides is possible. It is also possible that the lack of available hydration water in the gelatin matrix further contributes to the observed Tc(VI) stability.

Alkaline matrices were also observed to favor generation of Tc(VI). Studies probing the stability of $TcO_4{}^{2-}$ using fast scan rate cyclic voltammetry and pulse radiolysis showed the lifetime of $TcO_4{}^{2-}$ is in excess of 10 ms in moderately alkaline conditions (0.1 M OH⁻) albeit no detailed information regarding its stability has been reported.[59,60] The above observations point to the fact that in alkaline, high ionic strength matrices, the lower availability of free water for hydration/hydrolysis in high ionic strength aqueous matrices combined with the lower dissolved oxygen content therein, can enhance the stability of Tc(VI) species.

Based on kinetic studies in moderately alkaline conditions, Founta et al.[58] proposed that the reduction of Tc(VII) to Tc(V) goes through a Tc(VI) intermediate in either a disproportionation or an ECE mechanism with the following initial steps.

$$TcO_4^- + e^- \rightleftharpoons TcO_4{}^{2-} \quad E° = -0.88V \text{ vs. SCE} \quad [1]$$
$$TcO_4{}^{2-} + H_2O \rightleftharpoons TcO_3OH^- + HO^- \quad [2]$$
$$TcO_3OH^- + H_2O \rightarrow TcO_2(OH)_3{}^- \quad [3]$$

Examination of the kinetic dependence of the above mechanism suggests that the persistence of Tc(VI) should increase under highly alkaline conditions, as well as with high ionic strengths depending upon the rate determining step. Alkaline matrices promote a Tc(VI) product if step [3] is the rate determining step, while high ionic strength matrices would stabilize a Tc(VI) species if step [2] is the rate

determining step. Furthermore, careful monitoring of the decomposition kinetics as a function of pH shows the disproportionation rate to be maximum around pH = 8 to 9 and significantly lower at acidic or alkaline pH.[61] Persistence of Tc(VI) has been observed to significantly increase in alkaline solutions upon increasing the caustic concentrations from 0.001 M NaOH to 0.10 M.[57,61] Thus a change in the kinetic rate, and the exact nature of the rate determining step, i.e. a change from equation (3) to equation (2), in the above mechanism may occur at very high alkalinity or acidity.

A combination of these observations allowed us to propose the enhanced stabilization of Tc(VI) intermediate in alkaline, high-ionic strength solutions. This study demonstrates by spectroelectrochemical and spectroscopic techniques that Tc(VI) species in high ionic strength alkaline solutions can have a lifetime six orders of magnitude greater than previously observed. These observations coupled with the literature reports of stabilization of Tc(VI) species in high ionic strength, alkaline solutions and in the presence of ligand mixtures suggests that in aqueous solutions typified by these conditions, Tc(VI) can be a significant contributing factor to the redox speciation of Tc.

While increasing the fundamental understanding of Tc redox chemistry under these high ionic conditions is a noble pursuit in of itself, the knowledge gained through this understanding can have far-reaching impacts in the applied field of nuclear remediation. [99]Tc is generated as one of seven long-lived fission products from [235]U fission in nuclear reactors. The high chemical mobility and a half-life of 2.13 x 10^5 years of this isotope makes it a significant risk-driving contaminant in legacy nuclear waste, used nuclear fuel and contaminated subsurface plumes at their storage sites.[62] These systems are characterized by complex, high ionic strength matrices as well, where poor correlation of the observed and predicted Tc behavior based on the limited available thermodynamic models, solubility and redox speciation of Tc impedes design of successful remediation methods for legacy waste.[16,63] A determination of pertechnetate reduction behavior under highly alkaline and high ionic strength conditions, is necessary to understand the redox speciation of Tc under these conditions in order to facilitate design of effective remediation methods for nuclear waste streams. For this reason, the present study focuses on conditions relevant to legacy nuclear waste and utilizes a matrix of 5 M $NaNO_3$ with varied concentrations of NaOH. Our observation of the surprising stability of Tc(VI) in these matrices suggests an alteration of the reduction mechanism, and provides convincing evidence that Tc(VI) species may be highly relevant in Tc chemistry under these conditions.

Results

Cyclic voltammetry

The cyclic voltammetry of TcO_4^- was investigated in a 5 M $NaNO_3$ matrix with concentrations of NaOH varying from 0 M to 2 M on a glassy carbon working electrode (Figure 2 and S1).
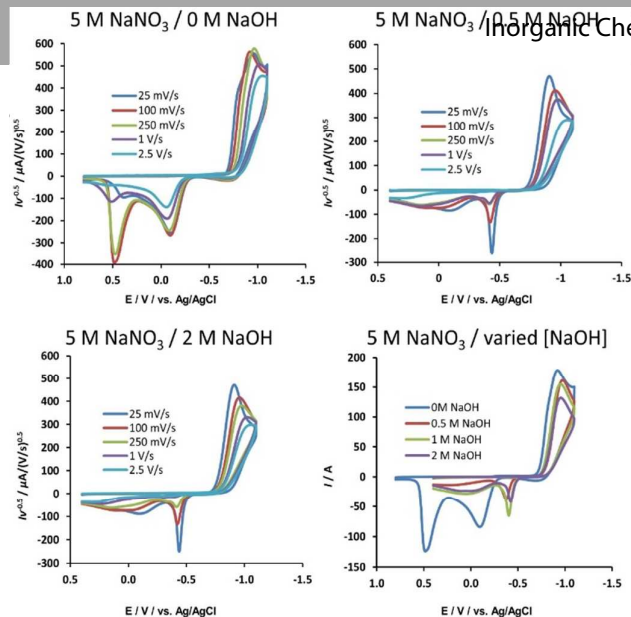
Figure 3. . Cyclic voltammograms of 5 mM TcO$_4^-$ in 5.0 M NaNO$_3$/0 – 2 M NaOH at variable scan rates 25-2500 mV s^{-1}, and an overlay of all conditions at 100 mV s^{-1}.

In 5 M NaNO$_3$/0 M NaOH, voltammograms at a scan rate of 25 mV s^{-1} display two overlapping electrochemically irreversible reductions. At faster scan rates, these became a single reduction peak which decreases in normalized peak current intensity and the band shifts progressively cathodic at rates above 250 mV s^{-1} suggesting sluggish heterogeneous electron transfer kinetics from the glassy carbon surface. The return wave shows an initial anodic peak at -0.17 V followed by a smaller peak at 0.4 V which increases in current with scan rate up until 250 mV s^{-1} when slow electron transfer kinetics are observed in the reduction peak.

When 0.5 M NaOH is introduced into the system, the voltammetric behavior changes considerably. The initial reduction at 25 mV s^{-1} is shifted negatively by approximately 75 mV and only displays a single reduction peak. Additionally, the reduction peak decreases in normalized peak current with increasing scan rate even at the moderate scan rates of 100 and 250 mV s^{-1}. The return sweep also shows dramatic differences with a sharp anodic feature at -0.46 V that rapidly decreases with scan rate. The increased sharpness the initial anodic wave with the introduction of hydroxide suggests that the hydroxide is encouraging the reduced species to precipitate or otherwise adhere to the electrode surface. This is followed by a drawn out oxidation that also decreases in current with increasing scan rate. The observed variation of anodic processes with scan rates (Figures S2 and S3) is consistent with what has been previously observed in hydroxide solutions on a Pt electrode.[56] The voltammetric results were found to behave similarly in solutions of up to 2 M NaOH, and all showed less current than voltammograms of the solution with identical TcO$_4^-$ concentration in a 5 M NaNO$_3$ matrix in the absence of hydroxide.

Voltammograms were simulated utilizing DigiElch V 7.0 software. The simulations over a range of scan rates satisfactory reproduce a 1e$^-$ process followed by a fast chemical step (as evidenced by an electrochemical irreversible process at up to 10 V s^{-1}) and more complex oxidation processes (Figures S4 and S5). The lack of electrochemical

reversibility leads to the hypothesis that Tc(VI) is not stable under these conditions as a tetrahedral oxo TcO$_4^{2-}$ species of similar geometry to TcO$_4^-$, but that if Tc(VI) persists, it must be in another chemical form.

Spectroelectrochemistry

While voltammetric studies strongly suggest a 1e$^-$ reduction, coulometric methods were not quantitative in determining the electron transfer stoichiometries due to insufficient separation of electrochemical processes and the edge of the solvent window on a Pt-gauze electrode. Therefore, UV-visible spectroelectrochemistry coupled with Nernstian analysis was performed to determine the stoichiometry of the electron transfer.

To evaluate the spectroelectrochemical behavior of TcO$_4^-$ in 5 M NaNO$_3$/2 M NaOH solution, double potential step chronoabsorptometry assisted with UV-visible absorption spectroscopy was employed. In a typical experiment, the initial potential was set to 0 V to ensure that the entire Tc concentration in the sample was in the fully oxidized TcO$_4^-$ state. The absorbance at 440 nm was concurrently recorded to establish a spectral baseline for the determination of the ingrowing reduced species. The working electrode potential was then set to a given value (E_{app}), and the solution was allowed to reach equilibrium, which was inferred when the UV-visible absorption spectrum no longer changed over a 3–4 min period.[64] Shown in Figure 3 are the absorption spectra at increasingly negative potentials as E_{app} was decreased in a stepwise fashion from the most positive to the most negative value. This allowed for measurement of the fully oxidized TcO$_4^-$ and fully reduced forms, as well as intermediate mixtures. At 0 V, the spectrum of TcO$_4^-$ only demonstrates a shoulder at approximately 350 nm. Figure 3a shows an overall increase in the intensities of the entire spectral region from 340-800 nm, highlighted by a progressive growth of a band centered at 440 nm, along with a simultaneous build-up of the intensity of a shoulder at ~657 nm. Reversing the coulometric step direction
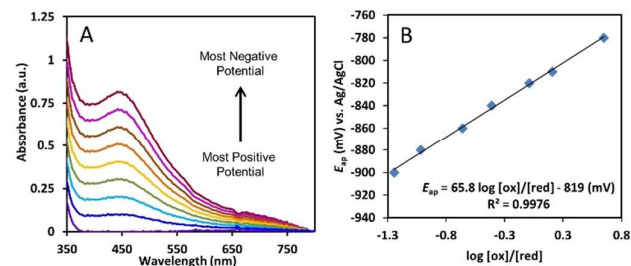

Figure 2. (A) Absorption spectra of 10.0 mM NH$_4$TcO$_4$ in an aqueous solution of 5 M NaNO$_3$/2.0 M NaOH recorded as a function of decreasing potential. The applied potentials are (—) -750 mV, (—) -780 mV, (—) -800 mV, (—) -820 mV, (—) -840 mV, (—) -860 mV, (—) -880 mV, (—) -900 mV and (—) -920 mV vs. Ag/AgCl. (B) Representative Nernst analysis done for the band at 440 nm for the redox process shown in Figure A. The equation for the analysis is: E_{app} (mV) = − (819±5) + (66±2) log [Ox]/[Red].

or varying the step size gave spectral changes that are consistent with the observed data. The spectroelectrochemical data resembled an [A]→[B] process, which motivated the analysis of the process according to the Nernst equation [4].

$$E_{app} = E^{0'} + \frac{0.0591}{n} log \frac{[Ox]}{[Red]} \qquad [4]$$

where $E^{O'}$ is the formal electrode potential, n is the number of electrons transferred, [Red] and [Ox] are the respective concentrations of the fully reduced and fully oxidized species. The ratio [Ox] / [Red] at applied potential E_{app} was estimated from $(A - A_{red})/ (A_{ox} - A)$, where A is the absorbance at the wavelength of interest; A_{ox} is the absorbance of the fully oxidized species, which was estimated from the absorbance at the most positive value of E_{app} (E_{app} = -0.75 V vs Ag/AgCl; where [Ox]/[Red] > 1000); A_{red} is the absorbance of the fully reduced sample, which was estimated from the absorbance at the most negative value of E_{app} (E_{app} = -0.920 V; where [Ox]/[Red] < 0.001).[64]

A plot of E_{app} versus log([Ox]/[Red]) at 440 nm (Figure 3b) exhibits a linear correlation described by the equation [5].

$$E_{app}(mV)=\{ -819 + 66 \log([Ox]/[Red]) \} \quad\quad [5]$$
$$TcO_4^- \rightleftharpoons Tc^{VI} \quad 0.82 \text{ V vs. Ag/AgCl} \quad\quad [6]$$

The slope of 66 mV corresponds to passing 0.9 equivalents of electrons and suggests an electron transfer stoichiometry of 1. The formal potential for the redox process of -819 mV vs Ag/AgCl obtained from the y-intercept is slightly less negative than the $E^{O'}$ of -909 mV obtained by fitting the cyclic voltammetry performed on a glassy carbon working electrode. This discrepancy can be attributed to the slower electron transfer kinetics of glassy carbon electrodes in aqueous solutions than the Pt working electrode used in the spectroelectrochemical measurements causing a higher over-potential. It is however worth mentioning that this is a non-Nernstian process; therefore the stoichiometry of electron transfer obtained through Nernstian analysis of the spectroelectrochemical data can be used merely as a qualitative indicator and has to be substantiated through other characterization and analyses.

Beyond approximately -900 mV no further increase in the peak at 440 nm is observed, and there is deposition of black precipitate on the working electrode surface which further interferes with the UV-vis measurements and reduces the absorbance by obstructing the light path. This precipitate is presumably insoluble $Tc(IV)O_2 \bullet nH_2O$ formed by the reduction of the Tc(VI) species.

The observed initial 1e$^-$ redox behavior of TcO_4^- in alkaline 5 M $NaNO_3$ solutions over the time frame of these experiments is unusual as most studies of the reduction of TcO_4^- in aqueous solutions indicate a 2e- or 3e- reduction to form a Tc(V) or Tc(IV) species.[22] While there have been instances of 1e-reduction of TcO_4^- with extremely fast scan rate voltammetry and pulse radiolysis,[59,60] the Tc(VI) product has been regarded to be highly unstable particularly in aqueous media[21,22] or in organic solutions in presence of atmospheric moisture[28] undergoing rapid disproportionation to Tc(VII) and Tc(V). Therefore, further spectral characterization studies were performed to confirm Tc(VI) oxidation state of the electro-reduction product.

Analysis of electrolytically generated species

In order to confirm the electrolytic formation of the Tc(VI) product, bulk electrolysis of 10 mM NH_4TcO_4 in the 5 M $NaNO_3$/2 M NaOH matrix was performed and resulted in brownish-purple coloration of the solution near the working electrode. Both the working electrode and the counter electrode solutions were carefully isolated to minimize their mixing. The room temperature electronic spectrum of the working electrode solution shows a dominant broad peak with a maximum of 440 nm and a smaller peak at approximately 657 nm. An additional shoulder observed at around 550 nm is poorly resolved. Detection of maxima below approximately 375 nm was not possible due to the large absorbance of nitrate. These features compare favorably with the diffuse reflectance spectrum of chemically prepared tetramethylammonium technetate, $(Me_4N)_2TcO_4$, taken at 77K, which demonstrates bands at 768, 731, 697, 655, 500, 298, 285, and 257 nm.[29] In the same paper, the exact values for the room temperature diffuse reflectance spectrum are not reported, but a figure demonstrates that this spectrum is broadened with fewer maxima. Another report[60] exists for the spectrophotometric measurement of the technetate ion at pH 13 generated by pulse radiolysis. Maxima are reported at 500 and 340 nm, but it should be noted that the solution used in the report was of considerably lower ionic strength, and the measurement of the technetate species was taken rapidly after generation, which may not allow sufficient time for rearrangement / transformation to another quasi-stable Tc(VI) species. There also exist Tc(VI) nitride aminocarboxylate compounds which exhibit a single λ_{max} at 505 nm.[51,52] Thus the maxima of 440, ~550, and 657 nm reported here is consistent with reports of similar Tc(VI) species.

The electrolysis product was also characterized by ^{99}Tc NMR and EPR spectroscopies. NMR can be effectively used for probing Tc species in the oxidation states +V and +VII. Tc in oxidation states of +IV and +VI can be probed using EPR spectroscopy as their monomeric forms are expected to have paramagnetic ground states. ^{99}Tc NMR of 10 mM TcO_4^- solution in 5 M $NaNO_3$/2 M NaOH before electrolysis showed a single sharp resonance at about 0 ppm (peak width = 10 Hz), characteristic of TcO_4^-.[57] The NMR spectrum of the working electrode solution isolated after bulk electrolysis showed a reduction in the intensity of the TcO_4^- resonance, with no appearance of other resonances to compensate for the reduction in TcO_4^- intensity. This is suggestive of partial conversion of pertechnetate to a paramagnetic species, which is no longer observable by NMR spectroscopy.

Figure 4 displays the EPR spectrum of the isolated working electrode solution at 125 K, showing a signal split into 10 lines, which can be attributed to hyperfine splitting due to the ^{99}Tc nucleus with a nuclear spin of 9/2. The fact that the signal is observed even at temperatures well above that of liquid helium, allows a Tc(IV) species to be ruled out as Tc S>1/2 spin systems are rarely observed at this temperature.[44,65] This suggests a S=1/2 technetium species,[65] which points to the formation of Tc(VI) during the electro-reduction process, as suggested by the Nernstian analysis. The spectrum increased in intensity as the temperature decreased and reached a maximum at approximately 40 K, whereupon the spectrum showed signs of power saturation. Fitting the spectrum with
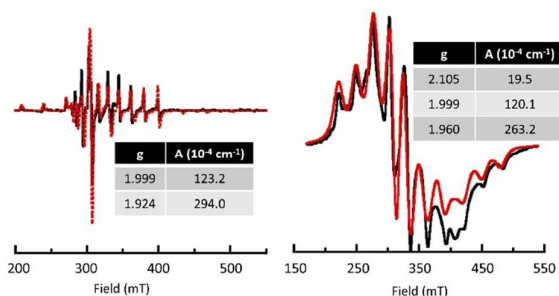
Figure 4. EPR spectra of (left) working electrode solution obtained by electro-reduction of 10 mM TcO_4^- in 5 M $NaNO_3$/2 M NaOH (T = 125 K) and (right) black precipitate deposited on the working electrode (T = 3.7 K). The dashed red line represents the experimentally obtained spectra, while the solid black line represents the Easyspin fit. The inset tables show the respective g and A parameters obtained from the fit.

Figure 5. Photoelectron spectra of Tc in (A) evaporated 1e⁻ electroreduction product and (B) electrodeposited black precipitate: (circles) experimental spectra, (blue trace) Tc(IV) fit based on literature, (red trace) Tc(VI) fit, (green trace) TcO_4^- fit based on literature, (grey trace) back ground and (brown trace) combined fit.

Easyspin yielded parameters typical for Tc(VI) compounds[36,37,39–42,47–49,65,66] – axial values for both Zeeman and hyperfine (allowing rhombicity yielded small deviations from axiality and concordantly small improvements in fit).

The observed g-values of g_1 = 1.999, and g_2 = 1.924 are similar to reported Tc(VI) literature values of $g_{//}$ and $g_\perp$ for $[TcOCl_5]^-$ of 2.057 and 1.938, for $[Tc(\mu\text{-}O_2Ar)]$ of g_{avg} = 2.0134, and for $[\{TcN(OH)(OH_2)\}_2(\mu\text{-}O_2)]$ of 1.892-2.0075 and 1.895-2.001 depending on acid strength.[40,49,66] The found $A_{//}$ and $A_\perp$ of 294 and 123 10^{-4} cm^{-1} also match literature values 230, and 96 10^{-4} cm^{-1} ($[TcOCl_5]^-$) and 344-363 and 163-174 10^{-4} cm^{-1} ($[\{TcN(OH)(OH_2)\}_2(\mu\text{-}O_2)]$).[40,66] Of all Tc(VI) EPR spectra reported in literature, these compounds likely have the most similar electronic structure to the quasi-stable Tc(VI) species seen in the present study. These values are also comparable to those reported for nitrido halide complexes which hover around g = 2.[38,67] While reports also exist of Tc(VI) compounds stabilized with thiolate ligands,[47–49] though due to the non-innocent nature of thiolates,[68] the electronic structure of the Tc(VI) center in these species is less likely to be similar to the Tc(VI) species generated in the present study.

Further electro-reduction of this Tc(VI) solution had generated a black precipitate. For its comprehensive analysis, bulk electrolysis was conducted at -1000 mV for 40 minutes to generate the precipitate electrodeposited on the working electrode surface in sufficient enough quantities for characterization. The platinum wire working electrode along with the precipitate was carefully removed from the electrolysis apparatus and analyzed by EPR spectroscopy. Variable temperature EPR was then acquired; however no spectrum became evident until the temperature was below 10 K. At 3.7 K, a broad signal was observed centered at ~3300 G, split again into approximately 10 lines. This spectrum matches closely to that reported by Lukens et al. for TcO_2 prepared in a variety of ways.[69] It should be noted that while this previous work reported spin Hamiltonian parameters from a simulation, our parameters are the results of least squares data-fitting.

XPS spectroscopic Analysis of Redox Products

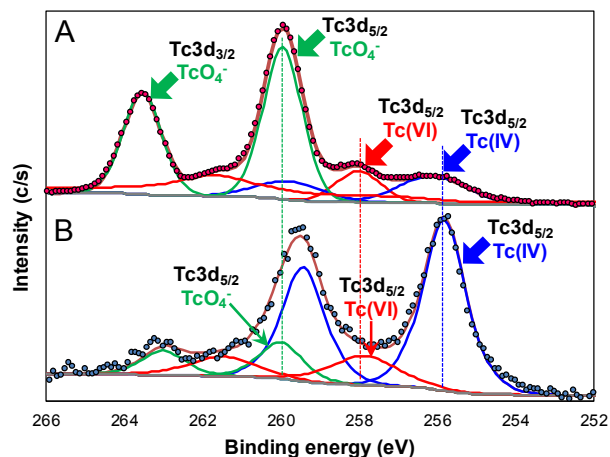To analyze the oxidation state of the electroreduction product using photoelectron spectroscopy, a drop of the isolated electrolyzed solution was placed on a carbon platform and allowed to evaporate under normal atmospheric conditions. The photoelectron spectrum of the solid residue left after evaporation exhibits three maxima originated from the overlap of three doublets whose lower binding energies were determined by the fitting at 259.9 eV, 258.0 eV and 256.1 eV as shown in Figure 5A. The binding energies of 259.9 eV and 256.1 eV are assigned to the $3d_{3/2}$ lines for Tc(VII) and Tc(IV) oxidation states respectively.[70,71] The remaining intermediate peak at 258.0 eV corresponds to a Tc in oxidation state lying between the above two. Literature reports of Tc photoelectron spectra are rare for oxidation states occurring between Tc(VII) and Tc(IV) with a Tc(V) species being the lone entry in the NIST XPS database (namely $[(n\text{-}C_4H_9)_4N]TcOCl_4$,[72] and Tc(VI) species being altogether absent thus far, to our knowledge. Therefore, the observed peak at 258.0 eV can be assigned to either a Tc(V) or a Tc(VI) oxidation state. It appears that the redox stability of this electrochemically generated intermediate species is greater than a Tc(V)-containing $[(n\text{-}C_4H_9)_4N]TcOCl_4$ species generated through an independent chemical synthetic step.[73] This is illustrated by the fact that the $[(n\text{-}C_4H_9)_4N]TcOCl_4$ product showed complete reduction to Tc(IV) in vacuum within 4 days; on the other hand, the electrochemical product preserved its stability even after 7 days. While the lack of XPS database prevents unambiguous assignment of the Tc oxidation state in the electrochemical product, it does not contradict the EPR and Nernstian analyses for the Tc(VI) assignment. It is noteworthy that the species is stable under atmospheric conditions in the solid state for at least 7 days.

The XPS spectrum for the electrodeposited black precipitate shown in Figure 5B (blue squares), shows the dominance of Tc(IV) oxidation state characterized by the peak with a lower binding energy of 256.1 eV. However, small fractions of the intermediate Tc oxidation state are also observed. A small portion of Tc(VII) is also observed presumably due to air

oxidation of either of the reduced products, or due to left over residual solution from the incomplete TcO_4^- reduction.

plot of the natural logarithm of Tc(VI) EPR intensity as a function of elapsed time, also shows a linear decay ($k = -0.363 \pm 0.013$/day), with a calculated half-life of a comparable 1.91 ± 0.07 days. These results in unison suggest the Tc(VI) product
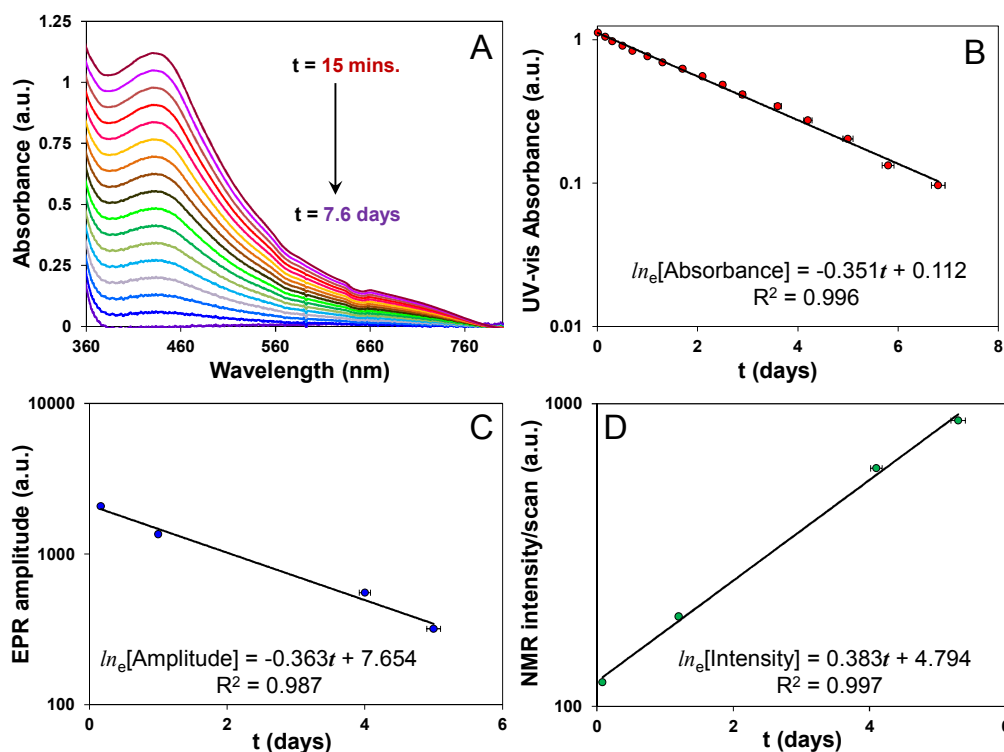

Figure 6. Kinetic stability of electrochemically generated Tc(VI) in an aqueous solution of 5 M NaNO₃/2 M NaOH monitored through various spectroscopic methods. (A) Overlaid UV-vis spectra recorded periodically after electrolytic generation of Tc(VI) from t = 15 mins (dark red trace) to t = 7.6 days (violet trace). (B) The natural logarithmic decay of the UV-vis absorbance maxima (λ_{max} = 445 nm) as a function of time; equation of the linear fit: ln_e[Absorbance] = -0.351t + 0.112, R^2 = 0.996. (C) The natural logarithmic decay of the EPR amplitude of the Tc(VI) species as a function of time; equation of the exponential fit: ln_e[Amplitude] = -0.363t + 7.654, R^2 = 0.987. (D) The natural logarithmic growth of the intensity of the ⁹⁹Tc NMR resonance corresponding to TcO_4^- with time; equation of the exponential fit: ln_e[Amplitude] = 0.383t + 4.794, R^2 = 0.997.

Kinetics of Tc(VI) decomposition.

The kinetic stability of the electrochemically generated Tc(VI) species in 5 M NaNO₃/2 M NaOH solution was monitored using three independent techniques including UV-visible, ⁹⁹Tc NMR and EPR spectroscopies. The UV-visible spectra of the solution isolated from the cathodic chamber of electrochemically generated Tc(VI) demonstrated a gradual reduction of the absorbance intensity over time (Figure 6). A plot of the natural logarithm of Tc(VI) absorbance as a function of elapsed time shows a linear decay, suggesting the decomposition to follow first-order kinetics in terms of Tc concentration ($k = -0.351 \pm 0.017$ /day). The half-life ($t_{1/2}$) of the Tc(VI) product under first order decomposition can be obtained from the decomposition kinetics using relation 7, and is calculated to be 1.98 ± 0.09 days.

$$t_{1/2} = \frac{\ln(2)}{k} \qquad [7]$$

Monitoring the Tc(VI) signal through EPR spectroscopy shows a similar progressive reduction of the Tc(VI) signal intensity. A

has significant stability in the 5 M NaNO₃/2 M NaOH matrix. Complimentary NMR studies conducted to gain insight into the mechanism of Tc(VI) decomposition show a progressive and quantitative ingrowth of a resonance at about 0 ppm due to TcO_4^- formation. The natural logarithm of the build-up of the TcO_4^- resonance intensity with time follows a linear growth profile, with a rate comparable to the Tc(VI) decay ($k = 0.383 \pm 0.011$/day) corresponding to $t_{1/2}$ of 1.81 ± 0.06 days. Observation of a small initial concentration of TcO_4^- is attributed to a slight mixing of the anodic and cathodic compartments of the spectroelectrochemical cell used for the experiment. No other resonances are observed.

Two mechanisms of decomposition can be envisioned: a disproportionation of the Tc(VI) product into Tc(V) and TcO_4^-, and an aerial oxidation of Tc(VI) to Tc(VII). Regardless which mechanism is in play, the kinetics of decomposition is slow enough to allow us to characterize the product in aqueous solutions. A comparison of the lifetime of our electrogenerated Tc(VI) product with that of 10 ms observed for a Tc(VI) product generated in a lower ionic strength matrix

(0.1 M OH$^-$) indicates the stability of the product in our product to be 6-orders of magnitude higher.[59,60]

Discussion

Results of the cyclic volumetric evaluation of TcO_4^- reduction, Nernstian analysis of the spectroelectrochemical signal, and structural spectroscopic analysis of the reduction product generated by bulk electrolysis are mutually consistent and present a case that under strongly alkaline high ionic strength conditions, a Tc(VI) species is electrochemically generated and is considerably longer lived than has been previously observed in literature.[59] It should however be noted that the previous literature study was specifically probing a tetrahedral TcO_4^{2-} species while the nominally 2 day half-life observed in the present study is likely due to a Tc(VI) species that has undergone a significant geometric rearrangement. Modeling of voltammograms obtained on a glassy carbon working electrode with DigiElch show that for the current response observed, a 1e- reduction followed by a fast chemical step and later re-oxidation is a possible electrochemical mechanism. All attempts of modeling the initial reduction with a multiple electron process involving fast chemical kinetics resulted in too large of a current at all scan rates. Thus if the literature mechanism is followed, then the second reduction must occur at an extremely slow rate.[58]

The Nernstian analysis of the spectroelectrochemical data suggested 1e- reduction, which is also consistent with the cyclic voltammetry results. However, the non-Nernstian nature of the overall process led us to treat the data with caution. Consequently, when interpreting our observations on the intermediate Tc species, the alternate possibilities of Tc(IV) or Tc(V) oxidation states were also considered and systematically ruled out prior to accepting the Tc(VI) oxidation state.

It is reasonable to conclude that the species responsible for the spectrophotometric peak at 440 nm is the same species responsible for the EPR signal due to the nearly identical half-lives. Examining the EPR data first, Tc(V) can be ruled out as a likely due to observance of the EPR signal at temperatures above those of liquid helium. While a triplet state could be envisioned for a Tc(V) compound, literature examples of Tc(V) compounds bound by oxygen are diamagnetic,[38,46,74] and in the event of a triplet ground state, Tc(V) compounds still do not show well-resolved EPR signals, even at low temperatures.[44] This leaves the likely oxidation state responsible for the EPR spectrum as either Tc(IV) or Tc(VI). It is rare to observe EPR signals for Tc(IV) at elevated temperatures due to the S = 3/2 ground state. A signal present at 125 K is however consistent with what has been observed for Tc(VI) compounds[49] which have S = ½. In fact, it is accepted that the only Tc oxidation states that show well resolved EPR signals above liquid helium temperatures are Tc(0), Tc(II) and Tc(VI).[65] While there have been reports of observance of Tc(IV) EPR signals at temperatures higher than liquid Helium temperatures, these have been limited to solid Tc(IV) species incorporated within crystalline matrices alone, where lattice effects can be anticipated to influence the spin relaxation rates. Two

representative examples are $K_2[TcF_6]$–$K_2[PtF_6]$ mixed crystals and polycrystalline Tc(IV) embedded within a Sn-Al-PO_4 matrix.[75,76] There have been no reports to our knowledge of Tc(IV) being observed in frozen glass at higher-than-liquid-Helium temperatures.

In the spectroelectrochemical study, the stoichiometric number of electrons being passed could be consistent with either direct formation of Tc(VI) or slow formation of either Tc(V) or Tc(IV) produced via disproportionation. However, in the event of slow production of Tc(IV) via disproportionation, an initial rise in the visible spectrum after the completion of electrolysis would be anticipated. The lack of this observation allows us to rule out this possibility.

The presence of an intermediate oxidation state of either Tc(V) or Tc(VI) is also confirmed by XPS. Due to the scarcity of Tc(V) and Tc(VI) XPS spectra in the literature, assignment of the exact oxidation state is not possible at this time, but a persistent intermediate oxidation state is confirmed. This signal is being attributed to a Tc(VI) species on account of the Tc(V) species not adequately explaining the presence of the EPR signal. However, it should be kept in mind that evaporation of the solution during XPS ssample preparation and subsequent exposure to atmospheric conditions could affect the disproportionation of Tc(VI) leading to a mixture of Tc(IV), Tc(V) and Tc(VII).

The kinetic stability of Tc(VI) products upon electro-reduction in the present study is considerably higher than what has previously been observed,[59,60] but neither is it inconsistent with the literature. The previous pulse radiolysis studies were specifically probing the tetrahedral TcO_4^{2-} species, while the presently observed Tc(VI) species could likely be from one of the intermediate Tc(VI) species seen in equations 2 or 3 that were presented by Founta et al.[58] The likely explanations for why this intermediate might be trapped: (a) the high ionic strengths in solution, (b) the binding of a ligand, such as nitrate, to the Tc(VI) product, (c) the high concentration of OH$^-$ in the present study, or some combination thereof. In the present scenario, the increase in hydroxide concentration is the most likely explanation as the voltametric behavior of all solutions containing hydroxide behave similarly, while the 5 M $NaNO_3$/0 M NaOH solution showed considerably different behavior. This would presumably mean equation [3] to be the rate determining step in the alkaline high-ionic strength conditions. Examination of the literature mechanism is consistent with this interpretation. The rate determining step could be shifted to the equation [2] in general high ionic strength matrices or in acidic solutions, which is protonation of TcO_4^{2-}. Therefore, one possible explanation for the different redox behavior between neutral nitrate solutions and highly alkaline nitrate solutions is that under highly alkaline high ionic strength conditions, reaction (2) replaces reaction (3) as the rate-determining step.

The second explanation would involve reaction of the reduction product (2) with a ligand present in solution, to form a species such as $TcO_3(OH)(NO_3)^{2-}$ blocking reaction (3). An analogous argument for peptide and protein binding may be

the missing explanation of why the Tc(VI) oxidation state is found to be more stable in the presence of gelatin.

Furthermore, formation of Tc(VI) consistent with the results of previous investigations to develop a spectroelectrochemical sensor for TcO_4^- detection by using polymer thin films on ITO electrodes which observed electrochemical reduction of TcO_4^- to an intermediate oxidation state between TcO_4^- and TcO_2.[77] While the authors did not further investigate whether the species was Tc(V) or Tc(VI), they concluded that the intermediate oxidation state was stabilized by the high concentration of ions in the film. It is likely that these results could be explained by stabilization of a Tc(VI) species due to a high ionic strength in an O_2 deficient environment in the ionomeric film.

Regardless which explanation is the cause, the observed mechanism of TcO_4^- reduction and stabilization of Tc(VI) oxidation state in the concentrated highly alkaline solutions is important to the fundamental understanding of group 7 chemistry and has significant implications to the processing of alkaline brine-like legacy radioactive tank waste, which is known to have chelators such as EDTA, gluconate, and iminodiacetate. Formation of quasi-stable Tc(VI) intermediate can also pave new directions for the development of electrochemical sensors for Tc.

Conclusions

The reduction mechanism of TcO_4^- to Tc(IV) has been shown in the literature to vary considerably with solution conditions. This has led to significant debate on the role and stability of the intermediate Tc(V) and Tc(VI) oxidation states. While the present study agrees with literature that reduction products of TcO_4^- eventually reoxidize to pertechnetate under ambient conditions, the lifetime of intermediate Tc(VI) oxidation state is found to be considerably longer than previously anticipated. The half-life of this species has been determined by both Visible and EPR spectroscopies to be nominally 2 days in aqueous solutions, while their stability is even higher when dry. Additionally, we report the rarely observed XPS and EPR signals of the Tc(VI) oxidation. This characterization of the otherwise unstable Tc(VI) oxidation state has large implications in the environmental chemistry of Tc. The isolation of Tc(VI) species under controlled potential reducing environments, and their stabilization in high ionic strength alkaline aqueous matrices is particularly relevant to Tc chemistry under environmental, biogeochemical and waste processing conditions, where the prevalent reducing conditions can be anticipated to stabilize Tc(VI), and thereby influence Tc speciation.

Conflicts of interest

There are no conflicts to declare.

Acknowledgements

Notes and references

1   M. I. Fokkema, L. J. M. de Heide, W. D. van Schelven and N. A. T. Hamdy, *Severe hypocalcaemia associated with extensive osteoblastic metastases in a patient with prostate cancer*, 2005, vol. 63.

2   R. Alberto, in *Medicinal Organometallic chemistry*, ed. J. Metzler-Nolte, Springer Berlin Heidelberg, 2010, pp. 221–246.

3   R. Alberto, R. Schibli, D. Angst, P. A. Schubiger, U. Abram and S. Abram, *Transit. Met. Chem.*, 1997, **22**, 597–601.

4   J. Terry, B. Grzenia, D. Papagiannopoulou, J. Kyger, S. Jurisson and J. D. Robertson, *J. Radioanal. Nucl. Chem.*, 2005, **263**, 531–537.

5   Mallinckrodt Inc., USA ., *PCT Int. Appl.*, 2001, 20 pp.

6   A. G. Jones, *Radiochim. Acta*, 1995, **70/71**, 289–297.

7   Mallinckrodt Medical, Inc., USA ., *PCT Int. Appl.*, 1998, 26 pp.

8   J. M. McBeth, J. R. Lloyd, G. T. W. Law, F. R. Livens, I. T. Burke and K. Morris, *Mineral. Mag.*, 2011, **75**, 2419–2430.

9   C. L. Thorpe, C. Boothman, J. R. Lloyd, G. T. W. Law, N. D. Bryan, N. Atherton, F. R. Livens and K. Morris, *Appl. Geochemistry*, 2014, **40**, 135–143.

10   N. K. Masters-Waage, K. Morris, J. R. Lloyd, S. Shaw, J. F. W. Mosselmans, C. Boothman, P. Bots, A. Rizoulis, F. R. Livens and G. T. W. Law, *Environ. Sci. Technol.*, 2017, **51**, 14301–14310.

11   L. Newsome, A. Cleary, K. Morris and J. R. Lloyd, *Environ. Sci. Technol.*, 2017, **51**, 1595–1604.

12   F. Poineau, E. Mausolf, G. D. Jarvinen, A. P. Sattelberger and K. R. Czerwinski, *Inorg. Chem.*, 2013, **52**, 3573–3578.

13   J. E. Till, *Technetium Environ.*, 1986, **99**, 1–20.

14   R. Wildung, K. McFadden and T. Garland, *J. Environ. Qual.*, 1979, **8**, 156–161.

15   E. H. Schulte and P. Scoppa, *Sci. Total Environ.*, 1987, **64**, 163–179.

16   J. P. Icenhower, N. P. Qafoku, W. J. Martin and J. M. Zachara, *The Geochemistry of Technetium: A Summary of the Behavior of an Artificial Element in the Natural Environment PNNL-18139*, Richland, WA, 2008.

17   P. R. Dixon and D. B. Curtis, in *Geochemistry*, Springer Netherlands, Dordrecht, 1998, pp. 620–621.

18	T. Ishii and T. Sakuragi, *Radioisotopes*, 2006, **55**, 485–494.
19	G. Desmet and C. Myttenaere, *Technetium in the Environment*, Springer Netherlands, 2012.
20	R. Alberto, *Eur. J. Inorg. Chem.*, 2009, 21–31.
21	J. A. Rard, *J. Nucl. Radiochem. Sci.*, 2005, **6**, 197–204.
22	J. A. Rard, M. H. Rand, G. Anderegg and H. Wanner, *Chemical Thermodynamics of Technetium*, North Holland/Elsevier, Amsterdam, 1999.
23	M. Jovtschev, H. Koch and H. Kupsch, *Isot. Isot. Environ. Heal. Stud.*, 1975, **11**, 369–378.
24	A. J. Bard, R. Parsons and J. Jordan, *Standard Potentials in Aqueous Solutions*, IUPAC (Marcel Dekker, New York, USA, 1985.
25	C. D. Russell, *Int. J. Appl. Radiat. Isot.*, 1982, **33**, 883–889.
26	R. J. Magee and T. J. Cardwell, in *Encyclopedia of Electrochemistry of the Elements, Vol. II*, ed. A. J. Bard, Marcel Dekker, New York, 1974, pp. 125–189.
27	L. Astheimer and K. Schwochau, *J. Inorg. Nucl. Chem.*, 1976, **38**, 1131–1134.
28	K. Schwochau, L. Astheimer, J. Hauck and H.-J. Schenk, *Angew. Chem. Internat. Ed.*, 1974, **13**, 346–347.
29	L. Astheimer, J. Hauck, H. J. Schenk and K. Schwochau, *J. Chem. Phys.*, 1975, **63**, 1988–1991.
30	R. Colton, *Nature*, 1962, **193**, 872–873.
31	H. Selig, C. L. Chernick and J. G. Malm, *J. Inorg. Nucl. Chem.*, 1961, **19**, 377–381.
32	D. W. Osborne, F. Schreiner, K. Otto, J. G. Malm and H. Selig, *J. Chem. Phys.*, 1978, **68**, 1108.
33	H. Selig and J. G. Malm, *J. Inorg. Nucl. Chem.*, 1962, **24**, 641–644.
34	J. H. Holloway and H. Selig, *J. Inorg. Nucl. Chem.*, 1968, **30**, 473–478.
35	R. Colton and I. B. Tomkins, *Aust. J. Chem.*, 1968, **21**, 1981–1985.
36	J. Baldas, J. F. Boas and G. A. Williams, *Appl. Magn. Reson.*, 1996, **508**, 499–508.
37	J. Baldas, J. F. Boas, J. Bonnyman and G. A. Williams, *J. Chem. Soc. Dalt. Trans.*, 1984, 2395–2400.
38	J. Baldas, S. F. Colmanet and M. F. Mackay, *J. Chem. Soc. Dalt. Trans.*, 1988, 1725–1731.
39	R. Kirmse, K. Kohler, U. Abram, R. Bottcher, L. Golic and E. de Boer, *Chem. Phys.*, 1990, **143**, 75–82.
40	R. Kirmse, J. Stach and U. Abram, *Inorg. Chem.*, 1985, **24**, 2196–2198.
41	U. Abram, R. Hubener, R. Wollert, R. Kirmse and W. Hiller, *Inorganica Chim. Acta*, 1993, **206**, 9–14.
42	R. Kirmse, J. Stach and U. Abram, *Inorganica Chim. Acta*, 1986, **117**, 117–121.
43	U. Abram and R. Kirmse, *Radiochim. Acta*, 1993, **63**, 139–143.
44	R. Kirmse and U. Abram, *Isot. Isot. Enviromental Heal. Stud.*, 1990, **26**, 151–159.
45	A. J. Edwards, D. Hugill and R. D. Peacock, *Nature*, 1963, **200**, 672.
46	M. J. Abrams, V. S. K. Larsen and J. Zubieta, *Inorg. Chem.*, 1991, 2031–2035.
47	M. Kawashima, M. Koyama and T. Fujinaga, *J. Inorg. Nucl.*

	Chem., 1976, **38**, 801–805.
48	R. Kirmse, J. Stach and H. Spies, *Inorganica Chim. Acta*, 1980, **45**, L251–L253.
49	A. deLearie, Lynn, R. C. Haltiwanger and C. G. Pierpont, *J. Am. Chem. Soc.*, 1989, **111**, 4324–4328.
50	J. Boas, J. F. Boas, Z. Ivanov and B. D. James, *Inorganica Chim. Acta*, 1993, **204**, 199–212.
51	T. Takayama, Y. Kani, T. Sekine, H. Kudo and K. Yoshihara, *J. Radioanal. Nucl. Chem.*, 1995, **199**, 217–227.
52	T. Takayama, T. Sekine and K. Yoshihara, *J. Radioanal. Nucl. Chem., Lett.*, 1993, **176**, 325–331.
53	H. H. Miller, M. T. Kelley and P. F. Thomason, Pergamon, 1960, pp. 716–726.
54	K. Schwochau and L. Astheimer, *Zeitschrift fuer Naturforsch.*, 1962, **17a**, 820.
55	S. I. Zhdanov, A. F. Kuzina and V. I. Spitsyn, *Zhurnal Neorg. Khimii*, 1970, **15**, 803–806.
56	G. A. Mazzocchin, F. Magno, U. Mazzi and R. Portanova, *Inorganica Chim. Acta*, 1974, **9**, 263–268.
57	G. Kissel and S. W. Feldberg, *J. Phys. Chem.*, 1969, **161**, 3082–3088.
58	A. Founta, D. A. Aikens and H. M. Clark, *J. Electroanal. Chem.*, 1987, **219**, 221–246.
59	E. Deutsch, W. R. Heineman, R. Hurst, T. A. Mulac and S. Gordon, *J. Chem. Soc. Chem. Commun.*, 1978, 1038–1040.
60	K. Libson, J. C. Sullivan, W. A. Mulac, S. Gordon and E. Deutsch, *Inorg. Chem.*, 1989, **28**, 375–377.
61	S. V Kryuchkov, A. K. Pikaev, A. F. Kuzina and V. I. Spitsyn, *Dokl. Akad. Nauk SSSR*, 1979, **247**, 1187–90 [Phys. Chem.].
62	E. H. Schulte and P. Scoppa, *Sci. Total Environ.*, 1987, **219**, 221–246.
63	J. P. Icenhower, N. P. Qafoku, J. M. Zachara and W. J. Martin, *Am. J. Sci.*, 2010, **310**, 721–752.
64	C. A. Schroll, S. Chatterjee, W. R. Heineman and A. Bryan, 2012, 1065–1070.
65	U. Abram and R. Kirmse, *Radiochim. Acta*, 1993, **63**, 139–143.
66	J. F. Baldas, J. F. Boas, Z. Ivanov and B. D. James, *Inorganica Chim. Acta*, 1993, **204**, 199–212.
67	J. Baldas, J. F. Boas, S. F. Colmanet and M. F. Mackary, *Inorganica Chim. Acta*, 1990, **170**, 233–239.
68	R. Eisenberg and H. B. Gray, 2011, 9741–9751.
69	W. W. Lukens, J. J. Bucher, N. M. Edelstein and D. K. Shuh, *Environ. Sci. Technol.*, 2002, **36**, 1124–1129.
70	D. W. Wester, D. H. White, F. W. Miller, R. T. Dean, J. A. Schreifels and J. E. Hunt, *Inorganica Chim. Acta*, 1987, **131**, 163–169.
71	M. Thompson, A. D. Nunn and E. N. Treher, *Anal. Chem.*, 1986, **58**, 3100–3103.
72	D. W. Wester, D. H. White, F. W. Miller and R. T. Dean, *Inorganica Chim. Acta*, 1987, **131**, 163–169.
73	S. Chatterjee, A. Andersen, Y. Du, M. H. Engelhard, G. B. Hall, T. G. Levitskaia, W. W. Lukens, V. Shutthanandan, E. D. Walter and N. M. Washton, *PNNL-26265, EMSP-RPT-035 Characterization of Non-Pertechnetate Species Relevant to the Hanford Tank Waste*, Richland, WA, 2017.
74	A. Duatti, A. Marchi, L. Magon, E. Deutsch, V. Bertolasi and

G. Gilli, *Inorg. Chem.*, 1987, **26**, 2182–2186.

75   G. Roemelt and K. Schwochau, *Zeitschrift fuer Naturforschung, Tl. A Astrophys. Phys. und Phys. Chemie*, 1967, **22**, 519–522.

76   T. G. Levitskaia, S. Chatterjee, N. K. Pence, J. Romero, T. Varga, M. H. Engelhard, Y. Du, L. Kovarik, B. W. Arey, M. E. Bowden and E. D. Walter, *Environ. Sci. Nano*, 2016, **3**,

1003–1013.

77   D. J. Monk, M. L. Stegemiller, S. Conklin, J. R. Paddock, R. Heneman, William, C. J. Seliskar, T. H. Ridgway, S. A. Bryan and T. L. Hubler, in *ACS Symposium Series: Accomplishments of the Environmetal Management Science Program*, eds. E. Berkey and T. Zachry, Americ, Washington D.C., 2005.

For TOC only:
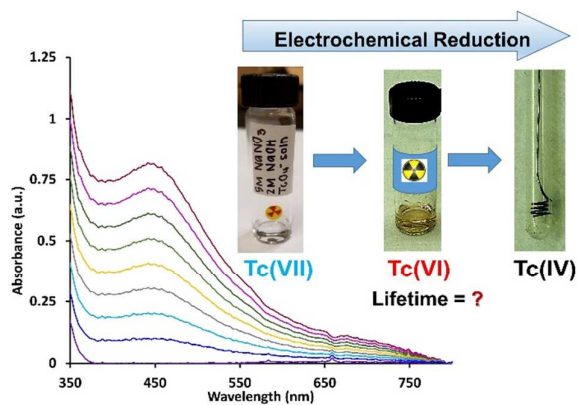
This work demonstrates an aqueous Tc(VI) lifetime 6 orders of magnitude greater than previously suggested.